nature cell biology

Myosin X regulates netrin receptors and functions in axonal path-finding

Xiao-Juan Zhu[1,4], Cheng-Zhong Wang[2,4], Peng-Gao Dai[1,4], Yi Xie[3], Ning-Ning Song[2], Yu Liu[1], Quan-Sheng Du[1], Lin Mei[1], Yu-Qiang Ding[2,5] and Wen-Cheng Xiong[1,5]

Netrins regulate axon path-finding during development, but the underlying mechanisms are not well understood. Here, we provide evidence for the involvement of the unconventional myosin X (Myo X) in netrin-1 function. We find that Myo X interacts with the netrin receptor deleted in colorectal cancer (DCC) and neogenin, a DCC-related protein. Expression of Myo X redistributes DCC to the cell periphery or to the tips of neurites, whereas its silencing prevents DCC distribution in neurites. Moreover, expression of DCC, but not neogenin, stimulates Myo X-mediated formation and elongation of filopodia, suggesting that Myo X function may be differentially regulated by DCC and neogenin. The involvement of Myo X in netrin-1 function was further supported by the effects of inhibiting Myo X function in neurons. Cortical explants derived from mouse embryos expressing a motor-less Myo X exhibit reduced neurite outgrowth in response to netrin-1 and chick commissural neurons expressing the motor-less Myo X, or in which Myo X is silenced using microRNA (miRNA), show impaired axon projection *in vivo*. Taken together, these results identify a novel role for Myo X in regulating netrin-1 function.

Axon path-finding is essential for proper wiring in the brain. During neural development, axons are navigated by extracellular guidance cues including netrins and repulsive guidance molecules (RGMs). DCC and neogenin, a family of immunoglobin domain-containing proteins, are netrin receptors[1–3]. Neogenin is also believed to be a receptor for RGMs[4,5]. Although DCCs do not have intrinsic catalytic activity, netrin-1 activates various signalling pathways, including cAMP, phosphatidylinositol-3 kinase, phospholipase C, MAPK, and RhoGTPase[6–12]. Recent studies indicate that DCCs interact directly with focal adhesion kinase (FAK)[13–15] and phosphatidylinositol transfer protein α (PITPα)[10]. These proteins seem to function in initiating netrin-1 intracellular signalling and regulating netrin-1 functions[10,11,13–15]. Nevertheless, exactly how neurite extension and axon navigation are regulated remains unclear. Here, we report a role for Myo X, an unconventional myosin implicated in cell adhesion and filopodia elongation, in DCC distribution and netrin-1-mediated neurite outgrowth and growth-cone guidance.

Myo X was identified by a yeast two-hybrid screening using the intracellular domain of neogenin as bait as this domain of DCC seemed to have intrinsic trans-activation activity[13,16]. Myo X contains a myosin tail homology 4 (MyTh4) domain and a band 4.1–ezrin–radixin–moesin (FERM) domain, and stimulates formation and extension of filopodia[17]. To determine the region of Myo X necessary for interaction, the binding activity of numerous Myo X constructs was examined. Myo X constructs containing the FERM domain (Myo $X^{\Delta Mo}$, Myo $X^{\Delta MoP}$, Myo $X^{\Delta MoPH}$ and Myo X^{tail}) and the FERM domain alone (Myo X^{FERM}) interacted with neogenin, whereas deletion of the FERM domain (Myo $X^{\Delta M\Delta F}$) abolished the interaction. Thus, the FERM domain was necessary and sufficient for interaction with neogenin. Similar results were observed in *in vitro* GST-pulldown assays (Fig. 1b) and in coimmunoprecipitation assays (data not shown). These data suggest that the intracellular domain of neogenin interacts with Myo X in a manner dependent on the FERM domain of Myo X.

The highly homologous cytoplasmic regions of neogenin and DCC contain three functionally important domains that are conserved across species: P1, P2 and P3 (Fig. 1c). Deletion of the P1 and P2 domains had little effect on binding to Myo X (Fig. 1c), suggesting that binding activity resided in the P3 domain. Deletion of the P3 domain abolished Myo X binding to neogenin and the P3 domain alone was sufficient for interaction with Myo X (Fig. 1c). The P3 domain-dependent interaction was also observed in *in vitro* pulldown assays and in mammalian cells (Fig. 1d, e). Taken together, these data indicated that DCC–neogenin interact with Myo X in yeast, *in vitro* and in mammalian cells in a manner dependent on the P3 domain of DCC–neogenin. It is noteworthy that DCC and neogenin semmed to have different binding affinity for Myo X. Neogenin associated more strongly with Myo X without the motor domain (Myo $X^{\Delta Mo}$) than with full-length Myo X, in both *in vitro* GST-fusion protein pulldown assays and in Cos-7 cells (Figs. 1b, d–f).

[1]Program of Developmental Neurobiology, IMMAG and Department of Neurology, Medical College of Georgia, Augusta, GA 30912, USA.
[2]Institute of Neuroscience and Key Laboratory of Neurobiology, Shanghai Institutes for Biological Sciences, Chinese Academy of Sciences, Shanghai 200031, China.
[3]Department of Pathology, University of Alabama at Birmingham, Birmingham, AL 35294, USA. [4]These authors contributed equally to this work.
[5]Correspondence should be addressed Y.-Q.D. or W.-C.X. (e-mail: dingyq@ion.ac.cn; wxiong@mcg.edu)

Received 10 October 2006; accepted 5 December 2006; published online 21 January 2007; DOI: 10.1038/ncb1535

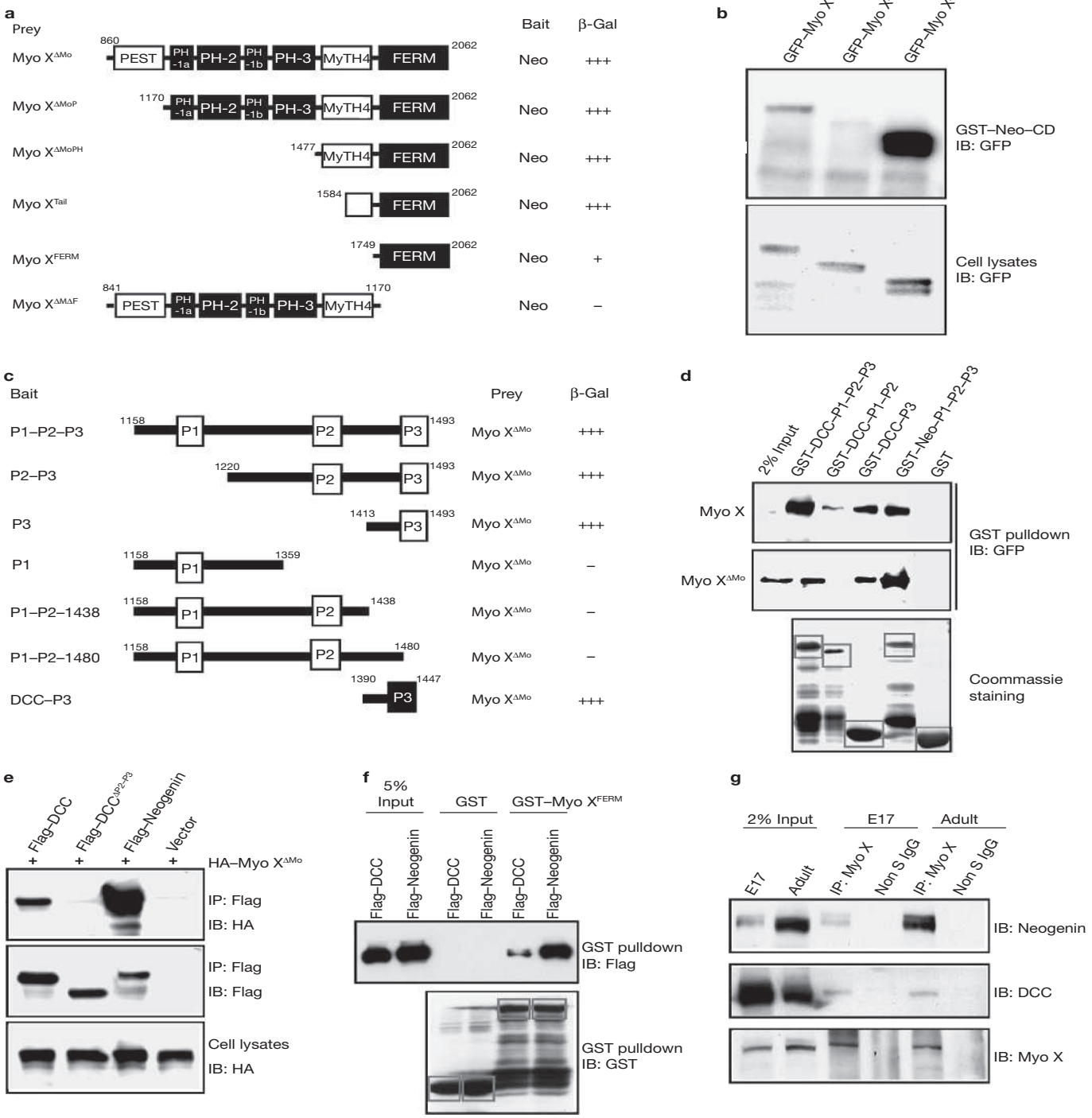

Figure 1 Myo X interaction with DCC and neogenin. (**a**) Requirement for the FERM domain of Myo X for binding to neogenin in yeast. (**b**) Neogenin interaction with the FERM domain of Myo X *in vitro*. (**c**) P3 domains in neogenin and DCC are essential for binding to Myo X in yeast. (**d**) *In vitro* interaction of Myo X with the P3 domain of DCC. (**e**) Coimmunoprecipitation of DCC and Myo $X^{\Delta Mo}$ in a manner dependent on the P3 domain. Cos-7 cells were transiently transfected with indicated plasmids. Cell lysates were incubated with anti-Flag antibodies to immunoprecipitate DCC or neogenin complexes, which were resolved on SDS-PAGE and immunoblotted with antibodies against Flag or HA. Myo $X^{\Delta Mo}$ in lysates was revealed by immunoblotting with anti-HA antibodies. (**f**) Differential binding affinity of the FERM domain for neogenin and DCC. (**g**) Myo X–DCC and Myo X–neogenin interaction in mouse brains. E17 and adult mouse brain homogenates (500 μg protein) were incubated with anti-Myo X (rabbit polyclonal) antibody and resulting immunocomplexes were probed with antibodies against DCC, neogenin and Myo X. Two percent of the input was included in the blot to indicate amounts of relevant proteins.In **a** and **c**, yeast cells were cotransformed with indicated constructs, seeded in $Leu^-Try^-His^-$ plates and scored as follows for β-gal activity: –, no blue after 24 h; +, blue in 4–8 h; +++, blue within 4 h. In **b**, **d** and **f**, Cos-7 cells expressing the indicated constructs were lysed and resulting lysates were incubated with indicated GST-fusion proteins (5 μg) immobilized on beads. Bound proteins were probed with anti-GFP or anti-Flag antibodies. GFP-fused Myo X or mutants in lysates were revealed by immunoblotting with anti-GFP antibodies (**b**). Similar amounts of different GST fusion proteins in **d** and **f** (indicated by boxes) were revealed by Coommassie blue staining (**d**) or immunoblotting with anti-GST antibody (**f**).

In contrast, DCC displayed seemingly greater binding affinity for full-length Myo X (Fig. 1d), suggesting differential regulation of Myo X by DCC and neogenin.

To characterize the interaction of endogenous Myo X and DCC–neogenin *in vivo*, a rabbit polyclonal antibody was raised against a peptide corresponding to amino acids 1004–1025 of mouse Myo X. This antibody was immunoreactive with two to three bands in lysates from neurons or rat brain, consistent with previous studies[18]. The immunoreactivity was specific, as it can be blocked by pre-absorption of the antibody with the antigen (data not shown). Homogenates of mouse E17 and adult brains were incubated with the anti-Myo X antibody to purify associated proteins. DCC and neogenin were detected in the immunoprecipitates at both ages (Fig. 1g). This association was specific because neither DCC nor neogenin was detectable in precipitates with non-specific immune IgG (Fig. 1g). The interaction of Myo X with neogenin in mouse brains seemed to be stronger than that with DCC, consistent with results of *in vitro* binding experiments and coimmunoprecipitation studies in Cos-7 cells (Fig. 1b–f). This may be due to a relatively low level of the full-length Myo X, but high level of the head-less isoform of Myo X expressed in mouse brains (data not shown). Nevertheless, our results suggest that Myo X interacts with DCC and neogenin in mouse brains.

Myo X functions to transfer cargo proteins into filopodia[17]. In light of its binding to DCC, we hypothesized that Myo X may deliver DCC to filopodia. To examine this hypothesis, we determined whether Myo X regulates DCC subcellular localization. DCC was distributed evenly on the surface of Cos-7 cells when it was cotransfected with GFP (see Supplementary Information, Fig. S1a). Remarkably, coexpression with GFP–Myo X led to redistribution of DCC into puncta at the cell periphery, colocalizing with Myo X (see Supplementary Information, Fig. S1b). This event required Myo X–DCC interaction and the motor domain of Myo X. Myo X mutants unable to bind to DCC (for example, GFP–Myo $X^{\Delta tail}$) did not alter DCC surface distribution (see Supplementary Information, Fig. S1c). When cotransfected with Myo $X^{\Delta Mo}$, a mutant that lacks the motor domain but interacts with DCC (see Supplementary Information, Fig. S1), DCC did not form surface puncta, although it was partially colocalized with Myo X (see Supplementary Information, Fig. 1d).

We then characterized the effect of Myo X on DCC distribution in neurons. Rat cortical neurons were transfected with plasmids encoding GFP alone or GFP–Myo X fusion proteins. Distribution of endogenous DCC was visualized as previously described[13]. DCC was evenly distributed in young neurons (before stage 3), but localized as distinct puncta in neurites and soma of differentiated neurons[13]. Expression of GFP alone had no effect on this distribution pattern (Fig. 2a). However, in young neurons expressing GFP–Myo X, DCC was redistributed as puncta in neurites, colocalizing with Myo X (Fig. 2a–c). In contrast, GFP–Myo $X^{\Delta tail}$, which was unable to interact with DCC, did not alter DCC distribution in neurons though GFP–Myo $X^{\Delta tail}$ was distributed as puncta at the periphery of soma (Fig. 2a–c). Together with results from Cos-7 cells, these observations indicate a role of the DCC–Myo X interaction in DCC redistribution. To confirm whether redistributed DCC was at the tips of filopodia, the localization of Myo X, DCC and their relationship with filopodia (labelled by phalloidin) were examined in neurons expressing GFP–Myo X. Myo X (indicated by GFP) and DCC (stained with anti-DCC antibody, red) were both enriched at the tips of filopodia (indicated by phalloidin, blue; see Supplementary Information, Fig. S2).

Whether Myo X is necessary for DCC subcellular location in neurons was further investigated by suppression of Myo X expression using short interfering RNA. The miRNA interference constructs of Myo X were generated and tested for effects on Myo X expression. Transfection of *Myo X-1* miRNA and *Myo X-2* miRNA, but not control (a scrambled miRNA), inhibited expression of cotransfected Myo X in Cos-7 cells and endogenous Myo X in NLT (a GnRH neuronal cell line) and neurons (see Supplementary Information, Fig. S3a). *Myo X-1* miRNA was more potent than *Myo X-2* miRNA (see Supplementary Information, Fig. 3a) and was subsequently used for further studies. DCC was localized to punctae in the soma and neurites of differentiated neurons transfected with both the control miRNA and *Myo X-1* miRNA (Fig. 2d, e). However, DCC immunofluorescence intensity in neurites was significantly reduced in neurons transfected with *Myo X-1* miRNA (Fig. 2d, e). Taken together, these results suggest that Myo X may be involved in targeting DCC to neurites.

We then asked whether the interaction with DCC or neogenin regulates Myo X function. Overexpression of Myo X has been shown to increase the number and length of filopodia[19]. To determine whether this event is regulated by netrin or DCC, NLT cells were transfected with GFP–Myo X and plated on coverslips coated with collegen type I (Col I). Under these conditions, cells form Myo X-dependent filopodia[20]. Cells expressing GFP–Myo X exhibited numerous filopodia within 3 h of plating, with Myo X enriched at the tips of filopodia (Fig. 3a). Filopodia were nearly absent in cells transfected with GFP alone (Fig. 3e), in agreement with previous reports[19,20]. Endogenous DCC was detectable in Myo X-induced filopodia (Fig. 3a). Coexpression of DCC further increased the number and length of filopodia in comparison with cells expressing GFP–Myo X alone (Fig. 3a, b, d and e). In contrast, neogenin coexpression caused a reduction in the number and length of filopodia (Fig. 3c, d and e), suggesting a differential regulation of Myo X function by DCC and neogenin. Moreover, netrin-1 seemed to enhance the differential effect of DCC and neogenin. When stimulated with netrin-1, DCC and Myo X coexpressing NLT cells showed dramatic changes in cell morphology and formation of neurite-like filopodia, resembling differentiation (Fig. 3b). However, neogenin and Myo X coexpressing NLT cells spread out more in response to netrin-1 stimulation (Fig. 3c). Similar regulatory effects of DCC and neogenin were observed in Cos-7 cells (see Supplementary Information, Fig. S4). Taken together, these results indicate that Myo X redistributes DCC into filopodia and Myo X-mediated filopodia formation and extension could be further enhanced by coexpression of DCC, but not neogenin.

Filopodia are motile and adhesive cellular structures that act as sensors for cell movement and axon outgrowth and guidance[19]. We thus reasoned that Myo X may be involved in netrin-1-regulated neurite outgrowth and axonal projections. This hypothesis was tested using an *in utero* electroporation model. GFP or Myo $X^{\Delta Mo}$ was introduced to the cortex of embryonic day 15 (E15) mouse embryos by *in utero* electroporation. Two days later, cortical explants were cultured to characterize netrin-1 stimulation of neurite outgrowth. The structure of Myo $X^{\Delta Mo}$ resembles that of the motor-less splice isoform of Myo X, which is expressed in developing rat brains and whose function remains unclear[21]. We speculated that it may function as a dominant-negative mutant by preventing endogenous Myo X from binding to DCC, thus inhibiting the effect of netrin-1 on neurite outgrowth. Alternatively, it may act as a downstream mediator of neogenin, as it binds to neogenin with higher affinity (Fig. 1). Only a few short neurites grew from GFP-expressing

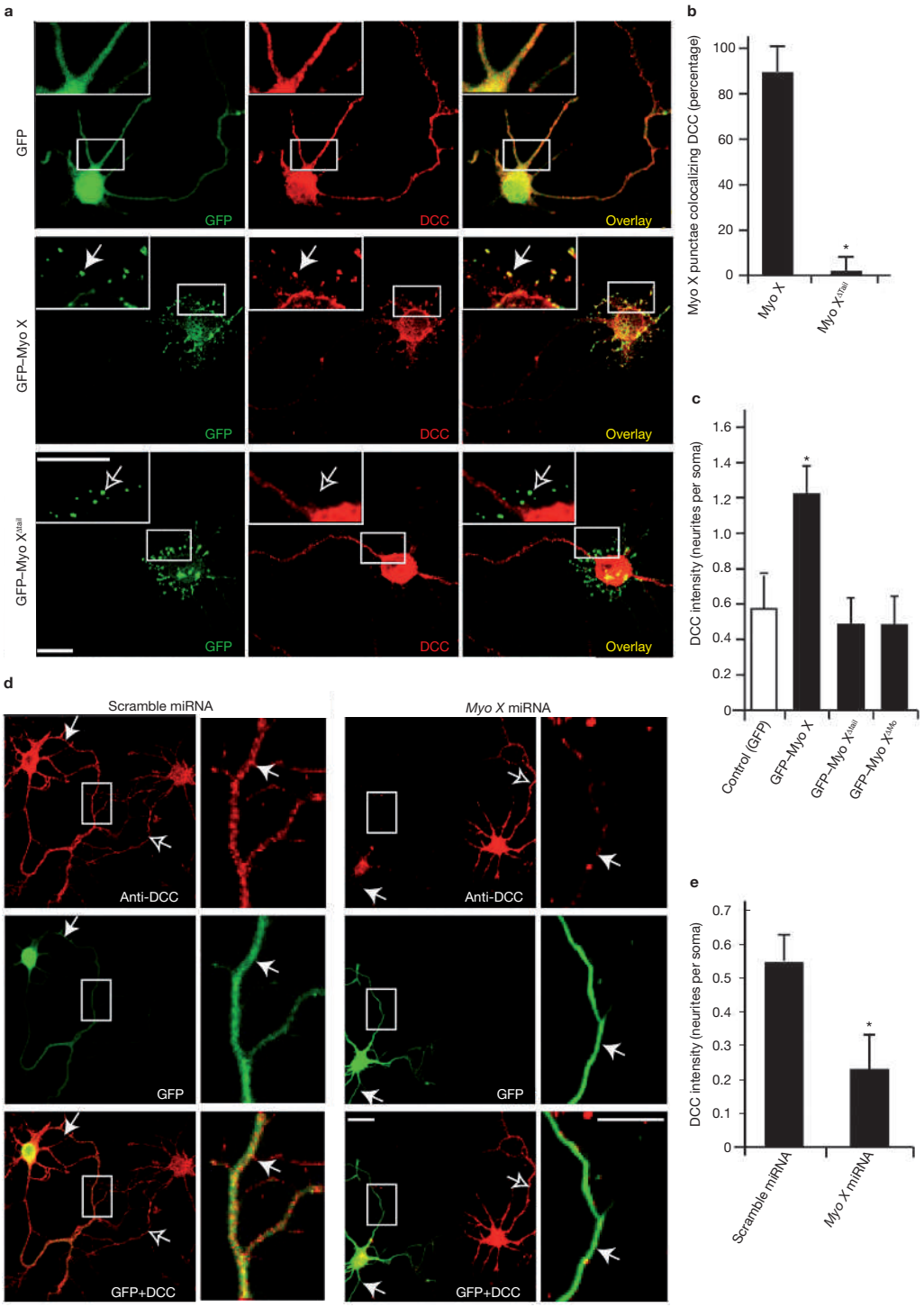

Figure 2 Regulation of DCC distribution in neurons by Myo X. (**a**) DCC redistribution in neurons expressing Myo X. Rat cortical neurons (E17, DIV 3) transfected with indicated GFP or GFP–Myo X plasmids were fixed and stained with antibodies against DCC for endogenous DCC distribution (red). GFP (green) indicated expression of GFP or GFP-fused Myo X proteins. The square boxes were magnified and are shown in the inserts. DCC–Myo X colocalizing puncta were indicated by filled arrows and the non-colocalized Myo X puncta were indicated by open arrows. (**b**, **c**) Quantification of data from **a**. In **b**, the percentage of GFP–Myo X and GFP–Myo $X^{\Delta Tail}$ puncta that colocalized with the endogenous DCC are presented as means ± s.e.m. ($n = 3$). The asterisk indicates $P < 0.01$, in comparison with cells expressing GFP–Myo X. In **c**, the ratio of DCC immunofluorescence intensity in neurites over soma are presented as means ± s.e.m. ($n = 10$). The asterisk indicates $P < 0.01$, in comparison with cells expressing GFP alone. (**d**) Reduced DCC distribution in neurites by suppression of Myo X expression. Rat cortical neurons (E17, DIV 7) transfected with control miRNA (scramble miRNA) or *Myo X* miRNA were fixed and stained with antibodies against DCC for endogenous DCC distribution (red). GFP indicates expression of transfected miRNA plasmids. The boxed areas were magnified and are shown in the right-hand panels. Transfected neurons are indicated by filled arrows and untransfected neurons are indicated by open arrows. (**e**) Quantification of data from **d**. The ratio of DCC immunoflourescence intensity in neurites over soma are presented as means ± s.e.m. ($n = 10$). The asterisk indicates $P < 0.01$, in comparison with neurons expressing scramble miRNA. The scale bars represent 50 μm in **a** and **d**.

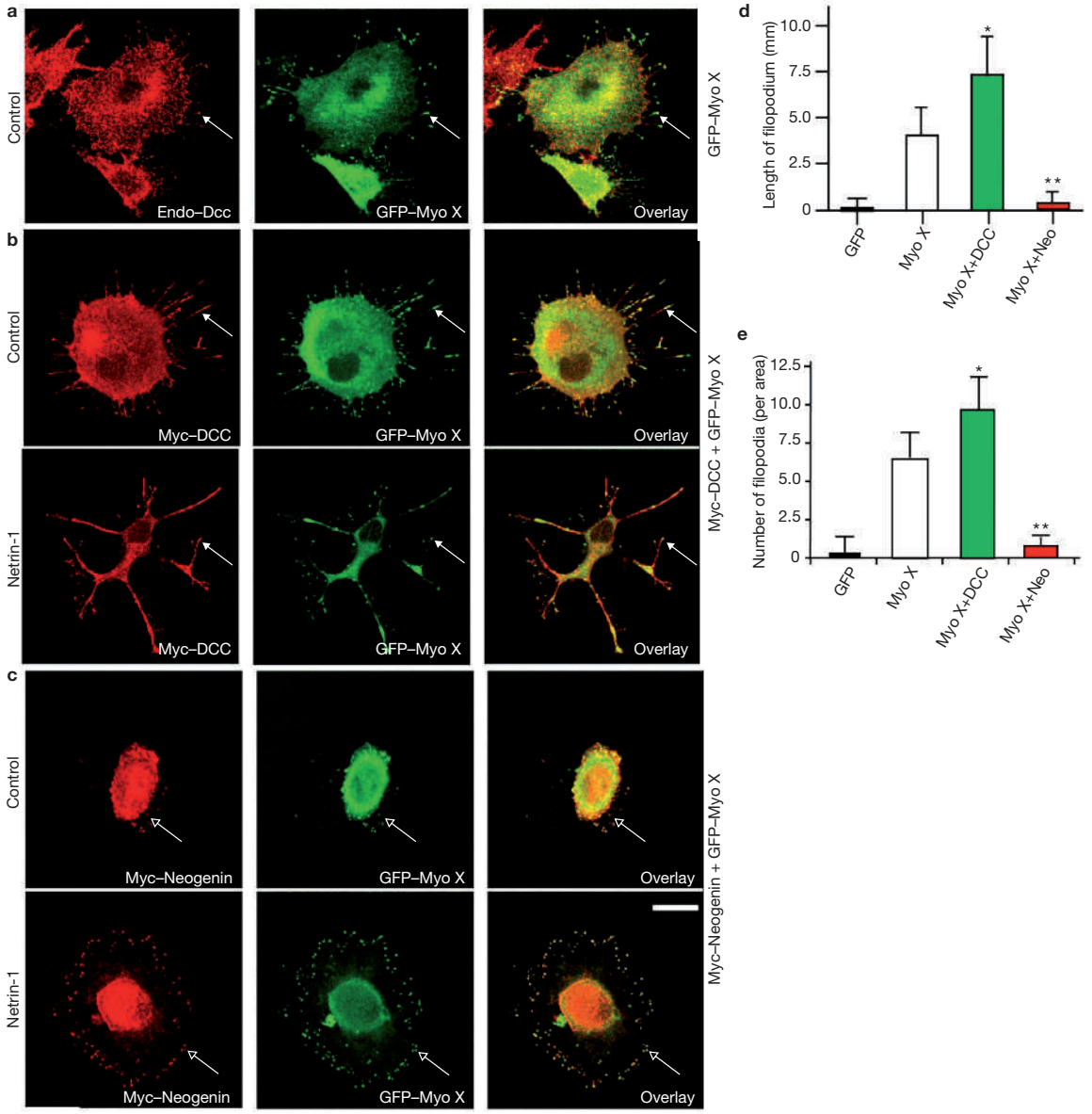

Figure 3 Distinct regulation by DCC and neogenin of Myo X-mediated filopodium elongation in NLT cells. (**a**–**c**) NLT cells were transfected with GFP–Myo X without (**a**) or with DCC (**b**) or neogenin (**c**). Transfected cells were plated onto collagen-coated coverslips for 3 h and treated with or without netrin-1 medium for 30 min. Cells were stained using anti-DCC or anti-Myc antibodies (red). GFP indicated Myo X expression. The scale bars represent 50 μm. (**d**, **e**) Quantification of filopodial lengths (**d**) and number (**e**) in NLT cells transfected with indicated plasmids without netrin-1 treatment. Data are presented as means ± s.e.m. (n = 30). Single asterisk indicates P <0.05 and double asterisk indicates P < 0.01, in comparison with cells expressing Myo X alone.

cortical explants in the absence of netrin-1 (Fig. 4a, c); the number and length of neurites were increased in explants stimulated by netrin-1, consistent with previous reports[22,23]. In contrast, netrin-1 stimulation of neurite outgrowth was nearly completely abolished in neurons expressing Myo $X^{\Delta Mo}$ in the cortical explants (Fig. 4b, c). This effect was not due to the death of neurons expressing Myo $X^{\Delta Mo}$, as they were TUNEL negative and survived in culture (data not shown). In addition, neurons not expressing Myo $X^{\Delta Mo}$ in the explants did respond to netrin-1, with an increased neurite outgrowth, as evident from phalloidin staining (Fig. 4b, c). Furthermore, netrin-1-independent neurite outgrowth (for example, treated with control medium) was also reduced in neurons expressing Myo $X^{\Delta Mo}$ (Fig. 4), suggesting the involvement of Myo X in neurite outgrowth in response to, but not limited to, netrin-1. It has also been demonstrated that Myo X is involved in integrin targeting in endothelial cells[20], and that integrin engagement is necessary for neurite outgrowth in this event.

We next investigated the role of Myo X in axonal projections *in vivo*. Myo $X^{\Delta Mo}$ was expressed in commissural neurons in chick neural tubes by *in ovo* electroporation, as axons of commissural neurons travel ventrally and then cross the midline in response to netrin-1. Commissural axons in chick spinal cord expressing GFP, an indicator of expressed plasmids, were located predominately on the contralateral side of the neural tube (Fig. 5a). In contrast, commissural axons expressing Myo $X^{\Delta Mo}$ failed to reach the contralateral ventral-horn region or to cross the midline

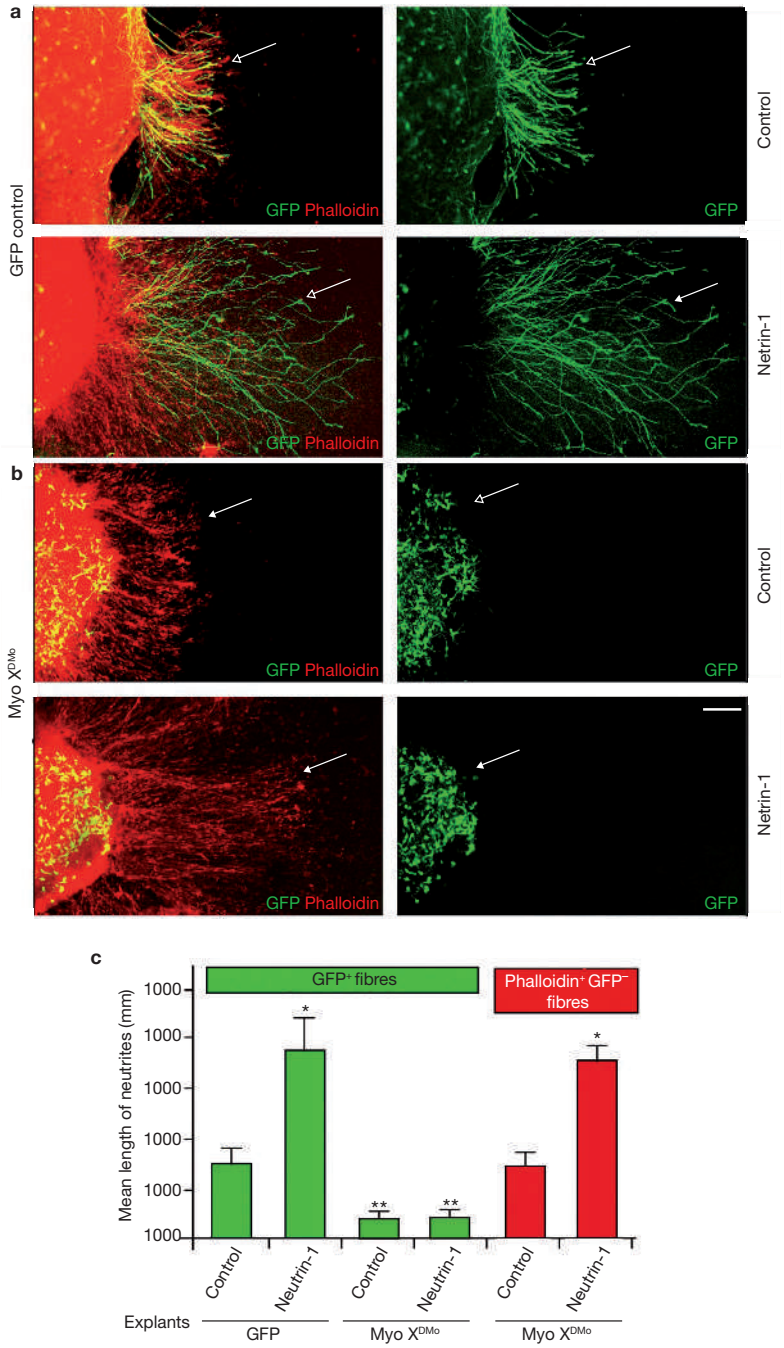

Figure 4 Involvement of Myo X in netrin-1-induced cortical neurite outgrowth. (**a**, **b**) Neurite outgrowth of cortical explants derived from mouse embryos expressing GFP control (**a**) or Myo $X^{\Delta Mo}$ (**b**) in response to netrin-1. Cortical explants (E17.5) of control (GFP) or Myo $X^{\Delta Mo}$ electroporated mouse embryos were cultured in matrigels with or without netrin-1 medium for 12 h. Explants were fixed and stained with phalloidin and anti-GFP antibody. Confocal microscopy images are shown. Neurite outgrowth in response to control (open arrows) or netrin-1 (filled arrows) is indicated. The scale bar represents 100 μm. (**c**) Quantification of data in **a** and **b**. GFP- or phalloidin-labelled neurite lengths per explant were measured (mean ± s.e.m.). Four explants from each group were analysed ($n = 4$). The single asterisk indicates $P < 0.05$ and the double asterisk indicates $P < 0.01$ (significantly different from control-treated GFP-expressing explants).

(Fig. 5a–c), implicating Myo X in commissural axonal projection to the contralateral side. Only neurons expressing Myo $X^{\Delta Mo}$ showed defects in axon projections and the commissural axonal projections of neurons without Myo $X^{\Delta Mo}$ expression were not affected (Fig. 5b). Moreover, expression of mutant Myo X proteins did not affect the generation of Lim 1/2- and Pax2-expressing interneurons, Isl1-expressing interneurons and motor neurons, or Pax 7-expressing dorso-ventral progenitors in the ventricular zone (data not shown; Lim1/2, Isl1, Pax2 and Pax7 are transcription factors and their expression was used to indicate the development of the spinal neural tube).

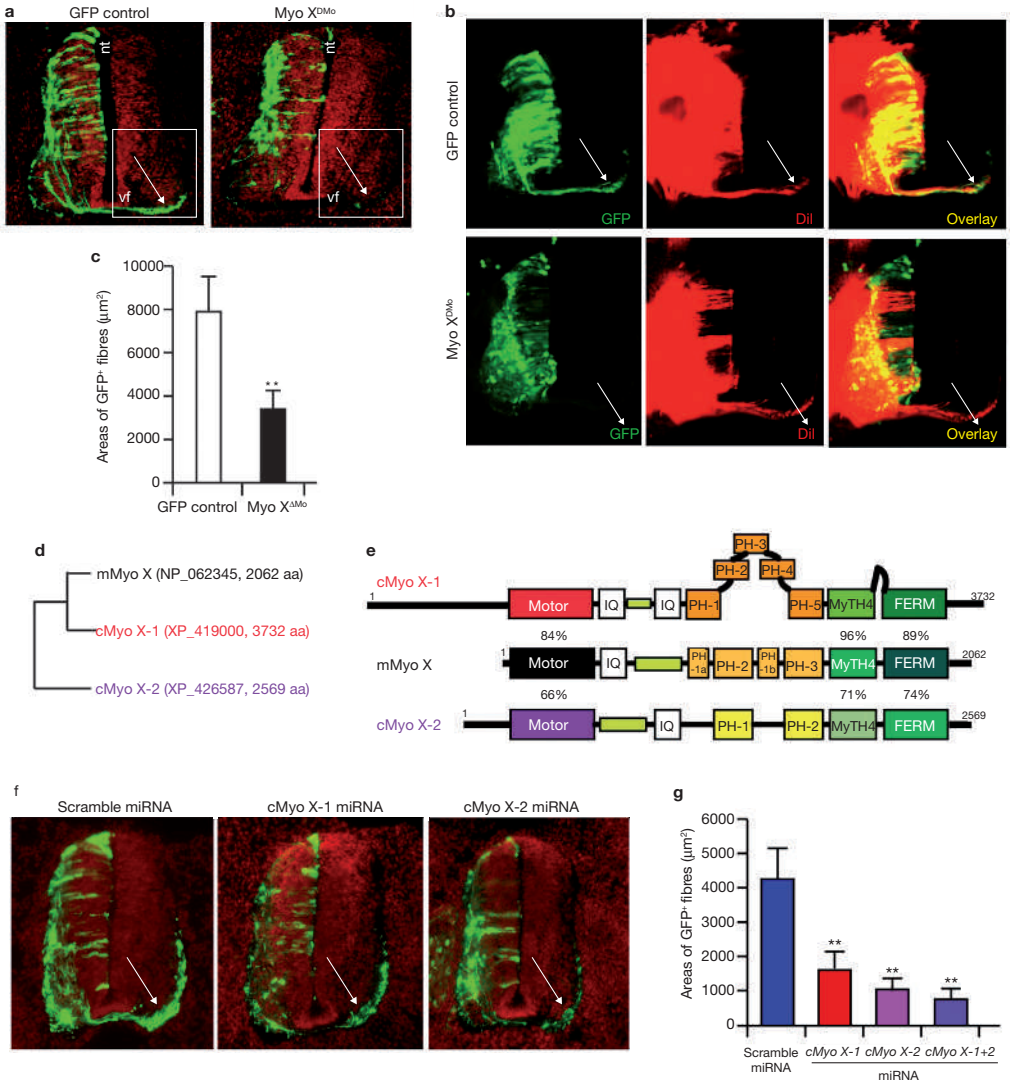

Figure 5 Impaired commissural neuronal axon projections in chicken embryos expressing motor-less Myo X or miRNA. (**a**, **b**) GFP-labelled (**a**) and GFP plus DiI-labelled (**b**) commissural axon tracts in chick embryos expressing indicated proteins following *in ovo* electroporation. Control and Myo $X^{\Delta Mo}$ plasmids, which contain an IRES element driving coexpression of GFP, were injected into the central canal of the neural tube of chick embryos at Hamburger and Hamilton (HH) stages 12–14. Electroporated embryos were then dissected out at HH stages 23–24, inserted with DiI, and examined for GFP expression and DiI labelling. Cross-sections are shown with dorsal to the top and ventral to the bottom. The ventral fasciculus (vf) and neural tube (nt) are indicated. (**c**) Quantification of data from the indicated area in **a**. Data are presented as means ± s.e.m. ($n = 40$). The double asterisk indicates $P < 0.01$ (different from control GFP). For quantification of the commissural axons on the contralateral side, the indicated areas (square boxes) of the GFP-positive axons (40 images, four images per embryo, total 10 embryos) were measured with MetaMorph software, 6.2. (**d**, **e**) Two chicken Myo X-related homologues were identified by BLAST searches of chicken genome data, cMyo X-1 (XP_419000, 3732 amino acids) and cMyo X-2 (XP_426587, 2569 amino acids). (**f**) Commissural axon tracts (GFP-labelled) in chick embryos expressing the indicated miRNA plasmids following *in ovo* electroporation. Arrows indicated a region with crossed fibres that were used for quantification in **g**. (**g**) Quantification of data from **f** (50 images, five images per embryo, total 10 embryos). Data are presented as means ± s.e.m. ($n = 50$). Double asterisks indicate $P < 0.05$ (significant difference from GFP control). The scale bars represent 100 μm.

The role of Myo X in axon guidance *in vivo* was examined using a complementary knockdown approach to suppress expression of endogenous Myo X in chicken embryos. Two chicken Myo X-related homologues were identified by BLAST searches of chicken genome data, cMyo X-1 (XP_419000, 3732 amino acids) and cMyo X-2 (XP_426587, 2569 amino acids; Fig. 5d, e). Plasmids, *cMyoX-1* miRNA and *cMyoX-2* miRNA (encoding miRNA against each *cMyo X*), were constructed and injected into the neural tube for *in ovo* electroporation. *cMyo X-1* miRNA and *cMyo X-2* miRNA specifically inhibited expression of *cMyo X-1* and *cMyo X-2*, respectively (data not shown). In the presence of either miRNAs, there was a reduction in commissural axons crossing to the contralateral side (Fig. 5f, g). Expression of both caused a further reduction (Fig. 5g), implicating overlapping function of cMyo X proteins in chick embryos. Taken together, these data demonstrate a role for Myo X in regulating commissural axonal projection in chick neural tubes.

In summary, we provide evidence of a role for Myo X in DCC distribution and netrin-1-guided axon projection. The interaction of DCC with Myo X enhances the formation and extension of filopodia, possibly as a consequence of increased local concentration of Myo X and its motor activity. Our results also provide insights into different effects

of netrin-1 stimulation of DCC and neogenin receptors. Whereas DCC plays an important role in mediating the attractive response to netrins, neogenin, as a receptor for RGMs, is implicated in repulsive functions[4,5,24]. Neogenin seemed to have a higher binding affinity for the motor-less/head-less Myo X variant (Myo $X^{\Delta Mo}$) compared with full-length Myo X. Thus, the motor-less/head-less Myo X splice variant (which occurs during development) would preferentially interact with neogenin, rather than DCC, and would have the ability to function as an inhibitor of DCC–Myo X signalling to prevent filopodia formation and to inhibit axon outgrowth. These observations are consistent with a recent report that, in *C. elegans*, MAX-1 (a protein that resembles the motor-less/head-less isoform of Myo X) is involved in the repulsion mediated byUnc5. another netrin receptor[25]. In addition, our observation that DCCs interact with the FERM domain of Myo X, the same region that binds integrins[20], raises the possibility of crosstalk between DCCs and integrins through regulation of Myo X in axon outgrowth and guidance. □

METHODS

Reagents and animals. Monoclonal antibodies were purchased as follows: anti-Flag from Sigma Chemical Co. (St Louis, MO); anti-Myc (9e10) from Santa Cruz (Santa Cruz, CA); goat anti-DCC from Santa Cruz. Rabbit polyclonal anti-neogenin was generated using GST-neogenin (amino acids 1158–1527) as antigens as described previously[10,13]. Rabbit polyclonal anti-Myo X was generated using mouse Myo X peptide sequences (DDDAFKDSPNPSEHGHSDQRTS) as antigens (NP_062345). Rabbit anti-Pax2 antibody was purchased from Zymed Lab (San Francisco, CA), and monoclonal antibodies against Isl1, Lim1/2, Nkx2.2, Pax6 and Pax7 were from the DSHB (Iowa City, IW).

Stable HEK 293 cells expressing human netrin-1 were previously described[26]. Unless otherwise indicated, ~200 ng ml^{-1} human netrin-1 was used for stimulation.

Yeast two-hybrid studies. The carboxy-terminal domain of neogenin (amino acids 1158–1527) was generated by PCR, subcloned downstream of the Gal4 DNA-binding domain in pGBT10 and used as bait to screen a mouse brain (oligo-dT-primed) cDNA library in pACT2 (refs 27, 28). The intracellular domain of DCC was self-activating (data not shown)[16]. Screens with the neogenin cytoplasmic domains identified clones that grew on plates lacking leucine, tryptophan and histidine with 25 μM 3-aminotriazole and were positive for β-galactosidase activity. The original clone encoded the C-terminal region of Myo X containing amino acids 841–2062 of mouse Myo X. Neogenin, neogenin mutants and the DCC-P3 domain were subcloned downstream of the GAL-4 DNA activation domain in pGAD424 as described previously[10,13].

Expression vectors. The cDNAs encoding *neogenin*, *DCC* or *DCC* mutants were amplified by PCR and subcloned into mammalian expression vectors downstream of a signal peptide and a Flag epitope tag (MDYKDDDDKGP) and under control of the *CMV* promoter[27]. The cDNAs of *Myo X* and mutants were subcloned into mammalian expression vectors (pEGFP) fused with GFP at the amino-terminus. The cDNA of *Myo* $X^{\Delta Mo}$ (dominant-negative Myo X) was also subcloned into the pCAGGS–IRES–EGFP vector for electroporation[29]. cDNA sequences corresponding to the cytoplasmic domains of DCC (amino acids 1108–1445), neogenin (amino acids 1158–1493) and Myo X (amino acids 1749–2062 for domain of FERM) were cloned into the pGEX-2T vector (Pharmacia) for GST fusion proteins. Deletion mutations in DCC, neogenin and Myo X were generated using the Quick Change kit (Stratagene, La Jolla, CA). The authenticity of all constructs was verified by DNA sequencing.

miRNA expression vectors were generated by the BLOCK-iT Lentiviral miR RNA Expression System (Invitrogen, Carlsbad, CA) according to the manufacturer's instruction. Briefly, *Myo X* sequence was analysed by a program provided by Invitrogen, and three regions were picked and cloned into pcDNA 6.2-GW–EmGFP-miR expression vector to yield pcDNA 6.2–GW/EmGFP-miR-Myo X. They were cotransfected with a HA-tagged Myo X construct into HEK 293 cells. Effective clones were identified based on their ability to suppress Myo X expression by western blot analysis and further confirmed by immunostaining. The sequences for the *Myo X* miRNA constructs are as follows: *Myo X* miRNA (mouse *Myo X*), 5′-TGCTGTTAATATCTTGGATCAGCTGCGTTTTGGCCAC TGACTGACGCAGCTGACAAGATATTAA-3′; *cMyo X-1* miRNA, 5′- TGCTGA AATAAGTTCCACAGAGTCTGGTTTTGGCCACTGACTGACCAGACTCTG GAACTTATTT-3′; *cMyo X-2* miRNA, 5′- TGCTGAAGACGTCCAGCCAACC ACATGTTTTGGCCACTGACTGACATGTGGTTCTGGACGTCTT-3′.

Cos-7 cell culture and transfection. Cos-7 cells were maintained in DMEM supplemented with 10% FCS, 100 units ml^{-1} penicillin G and streptomycin (GIBCO, Carlsbad, CA). Cells were plated at a density of 1×10^6 cells per 10-cm culture dish and allowed to grow for 12 h before transfection using the calcium phosphate precipitation method[13]. Thirty-six hours after transfection, cells were lysed in modified RIPA buffer (50 mM Tris–HCl at pH 7.4, 150 mM sodium chloride, 1% NP40, 0.25% sodium-deoxycholate and proteinase inhibitors)[27]. Lysates were subjected to immunoprecipitation or immunoblotting.

Protein–protein interaction assays. Immunoprecipitation was carried out as previously described[27]. Cell lysates (500 μg protein) were incubated with the indicated antibodies (1–2 μg) at 4 °C for 1 h in a final volume of 1 ml modified RIPA buffer with constant rocking. After the addition of protein A–G-agarose beads, the reactions were incubated at 4 °C for 1 h. Immune complexes were resolved by SDS–PAGE and subjected to immunoblotting. GST pulldown assay was carried out as described previously[27]. Transiently transfected HEK 293 cells were lysed in the modified RIPA buffer. Cell lysates were precleared with GST immobilized on glutathione–Sepharose 4B (Pharmacia, Piscataway, NJ) and then incubated with the indicated GST fusion proteins (2–5 μg) immobilized on glutathione–Sepharose beads at 4 °C for 1 h with constant rocking. The beads were washed three times with modified RIPA buffer, and bound proteins were resolved by SDS–PAGE and subjected to immunoblotting.

Cortical neuronal culture and immunostaining. Primary cortical neurons were cultured as described previously[13]. Briefly, embryos (E17) were removed from anesthetized pregnant Sprague-Dawley rats or mice. Cerebral cortices were dissected out and chopped into small pieces after meninges were completely removed. After incubation in PBS solution containing 0.125% (w/v) trypsin (Sigma) for 20 min at 37 °C, digested tissues were mechanically triturated by repeated passage through a Pasteur pipette in PBS solution containing 0.05% (w/v) DNase (Sigma). Dissociated cells were suspended in the neurobasal medium with B-27 supplement (Life Technologies, Carlsbad, CA) and 100 units ml^{-1} penicillin–streptomycin and were plated on poly-D-lysine coated dishes (Corning, New York, NY). After 2 days incubation at 37 °C in a 5% CO_2 atmosphere, 10 μM cytosine arabinoside was added to inhibit the proliferation of glial cells.

For immunostaining, E17 rat cortical neurons were cultured for 3 days (DIV 3) or 7 days (DIV 7) *in vitro* and processed for immunocytochemistry as previously described[13]. Briefly, cells were fixed with 4% paraformaldehyde or –20 °C methanol for 20 min, permeated, blocked with 5% bovine serum and incubated with antibodies against DCC (goat polyclonal, Santa Cruz) and Myo X (rabbit polyclonal). Double-labelled immunostaining was performed with appropriate fluorochrome-conjugated secondary antibodies. Images were taken on a Zeiss fluorescence microscope at 63×.

***In utero* electroporation and explant culture.** *In utero* electroporation was performed as previously described[30] with modifications. Timed pregnant wild-type mice at E14.5–E15.5 were anesthetized with intraperitoneal injection of sodium pentobarbital. After laparotomy, embryos were visualized through the uterus with a fibre-optic light source. The DNA solution (2.0 μg μl^{-1}), together with 0.1% Fast Green, was injected into the left lateral ventricle of each embryo through a glass capillary. The head of the embryo was placed between a pair of rectangular (3 × 5 mm) paddle-style electrodes and a series of five square-wave current pulses (33–35 V, 50 ms duration, at an interval of 950 ms) was delivered by a pulse generator (ECM830; BTX, San Diego, CA). The electrodes were positioned to aim for gene transfection in the dorsolateral wall of the hemisphere. The surgical incision in the mother was closed and embryos were allowed to develop *in utero*.

Explant assays were performed as described previously[22,31,32]. Embryos were dissected from the uterine horn of anesthetized pregnant mice. For cortical

explants, the telencephalic hemisphere of E16.5–E17.5 embryos was dissected out in L-15 medium and the pia was removed. The dorso-lateral cortex was cut with thin tungsten needles into approximately 200 × 200 μm pieces that spanned the full thickness of the cortical wall. Explants were embedded in a three-dimensional matrigel matrix with the ventricular side up. After polymerization, gels were incubated with neurobasal-B-27 medium (GIBCO) at 37 °C in a 5% CO_2 atmosphere. Explants were then fixed and stained with Texas red-conjugated phalloidin to label F-actin and with anti-GFP antibody to indicate GFP expression. Neurite outgrowth was analysed by immunofluorescence microscopy after 12–48 h in culture. Total neurite length (based on GFP or phalloidin staining) for each explant was obtained by adding the lengths of all neurites from each explant (regardless of bundle thickness). Four explants from each group indicated were analysed.

***In ovo* electroporation.** Fertilized chicken eggs were incubated at 38 °C under humid conditions for 50 h to HH stages 12–14 and 0.2 μl of plasmids (1.0 μg μl^{-1}) were injected into the central canal of the neural tube. After injection, plasmids were electroporated into one side of the neural tube with Electro Square Porator (ECM830; 25 V, 5 ms, 5 pulses). At HH stages 23–24, embryos were dissected out and sectioned transversely after fixation with 4% paraformaldehyde. For DiI labelling commissural axons, a tiny piece of DiI crystal was implanted into the dorsal neuronal tube on the electroporated side and placed in the fixative for 1 day at 37 °C. Commissural axons were observed by epifluorescence microscopy. For quantification of commissural axons on the contra-lateral side, areas of GFP-positive axons (40 images, 4 images per embryo, total 10 embryos) were measured by MetaMorph software, 6.2 (Downingtown, PA). Intensity of a pixel above 80 was considered to be positive. Data were analysed using a student's *t*-test.

Note: Supplementary Information is available on the Nature Cell Biology website.

ACKNOWLEDGEMENTS

This study was supported in part by grants from the National Institutes of Health (L.M. and W.C.X.), Muscular Dystrophy Association (L.M.), Philips Morris Research Program (L.M.), and National Nature Science Foundation of China (Y.Q.D. and W.C. X.).

AUTHOR CONTRIBUTIONS

All authors contributed to the experimental work and/or data analysis. Y.-Q.D. and W.-C.X. contributed to project planning.

COMPETING FINANCIAL INTERESTS

The authors declare that they have no competing financial interests.

Published online at http://www.nature.com/naturecellbiology/
Reprints and permissions information is available online at http://npg.nature.com/reprintsandpermissions/

1. Keino-Masu, K. *et al.* Deleted in Colorectal Cancer (DCC) encodes a netrin receptor. *Cell* **87,** 175–185 (1996).
2. Kolodziej, P. A. *et al.* frazzled encodes a *Drosophila* member of the DCC immunoglobulin subfamily and is required for CNS and motor axon guidance. *Cell* **87,** 197–204 (1996).
3. Chan, S. S. *et al.* UNC-40, a *C. elegans* homolog of DCC (Deleted in Colorectal Cancer), is required in motile cells responding to UNC-6 netrin cues. *Cell* **87,** 187–195 (1996).
4. Rajagopalan, S. *et al.* Neogenin mediates the action of repulsive guidance molecule. *Nature Cell Biol.* **6,** 756–762 (2004).
5. Matsunaga, E. *et al.* RGM and its receptor neogenin regulate neuronal survival. *Nature Cell Biol.* **6,** 749–755 (2004).
6. Ming, G. L. *et al.* cAMP-dependent growth cone guidance by netrin-1. *Neuron* **19,** 1225–1235 (1997).
7. Ming, G. *et al.* Phospholipase C-γ and phosphoinositide 3-kinase mediate cytoplasmic signaling in nerve growth cone guidance. *Neuron* **23,** 139–148 (1999).
8. Forcet, C. *et al.* Netrin-1-mediated axon outgrowth requires deleted in colorectal cancer-dependent MAPK activation. *Nature* **417,** 443–447 (2002).
9. Li, X., Saint-Cyr-Proulx, E., Aktories, K. & Lamarche-Vane, N. Rac1 and Cdc42 but not RhoA or Rho kinase activities are required for neurite outgrowth induced by the netrin-1 receptor DCC (Deleted in Colorectal Cancer) in N1E-115 reuroblastoma cells. *J. Biol. Chem.* **277,** 15207–15214 (2002).
10. Xie, Y. *et al.* Phosphatidylinositol transfer protein-α in netrin-1-induced PLC signalling and neurite outgrowth. *Nature Cell Biol.* **7,** 1124–1132 (2005).
11. Xie, Y. *et al.* DCC-dependent phospholipase C signaling in netrin-1-induced neurite elongation. *J. Biol. Chem.* **281,** 2605–2611 (2006).
12. Chang, C. *et al.* MIG-10/lamellipodin and AGE-1/PI3K promote axon guidance and outgrowth in response to slit and netrin. *Curr. Biol.* **16,** 854–862 (2006).
13. Ren, X. R. *et al.* Focal adhesion kinase in netrin-1 signaling. *Nature Neurosci.* **7,** 1204–1212 (2004).
14. Li, W. *et al.* Activation of FAK and Src are receptor-proximal events required for netrin signaling. *Nature Neurosci.* **7,** 1213–1221 (2004).
15. Liu, G. *et al.* Netrin requires focal adhesion kinase and Src family kinases for axon outgrowth and attraction. *Nature Neurosci.* **7,** 1222–1232 (2004).
16. Hu, G. *et al.* Mammalian homologs of seven in absentia regulate DCC via the ubiquitin-proteasome pathway. *Genes Dev.* **11,** 2701–2714 (1997).
17. Sousa, A. D. & Cheney, R. E. Myosin-X: a molecular motor at the cell's fingertips. *Trends Cell Biol.* **15,** 533–539 (2005).
18. Berg, J. S., Derfler, B. H., Pennisi, C. M., Corey, D. P. & Cheney, R. E. Myosin-X, a novel myosin with pleckstrin homology domains, associates with regions of dynamic actin. *J. Cell Sci.* **113,** 3439–3451 (2000).
19. Berg, J. S. & Cheney, R. E. Myosin-X is an unconventional myosin that undergoes intrafilopodial motility. *Nature Cell Biol.* **4,** 246–250 (2002).
20. Zhang, H. *et al.* Myosin-X provides a motor-based link between integrins and the cytoskeleton. *Nature Cell Biol.* **6,** 523–531 (2004).
21. Sousa, A. D., Berg, J. S., Robertson, B. W., Meeker, R. B. & Cheney, R. E. Myo10 in brain: developmental regulation, identification of a headless isoform and dynamics in neurons. *J. Cell Sci.* **119,** 184–194 (2006).
22. Metin, C., Deleglise, D., Serafini, T., Kennedy, T. E. & Tessier-Lavigne, M. A role for netrin-1 in the guidance of cortical efferents. *Development* **124,** 5063–5074 (1997).
23. Braisted, J. E. *et al.* Netrin-1 promotes thalamic axon growth and is required for proper development of the thalamocortical projection. *J. Neurosci.* **20,** 5792–5801 (2000).
24. Culotti, J. G. & Merz, D. C. DCC and netrins. *Curr. Opin. Cell Biol.* **10,** 609–613 (1998).
25. Huang, X., Cheng, H. J., Tessier-Lavigne, M. & Jin, Y. MAX-1, a novel PH/MyTH4/FERM domain cytoplasmic protein implicated in netrin-mediated axon repulsion. *Neuron* **34,** 563–576 (2002).
26. Li, H. S. *et al.* Vertebrate slit, a secreted ligand for the transmembrane protein roundabout, is a repellent for olfactory bulb axons. *Cell* **96,** 807–818 (1999).
27. Ren, X. R. *et al.* Regulation of CDC42 GTPase by proline-rich tyrosine kinase 2 interacting with PSGAP, a novel pleckstrin homology and Src homology 3 domain containing rhoGAP protein. *J. Cell Biol.* **152,** 971–984 (2001).
28. Wang, Q. *et al.* Regulation of the formation of osteoclastic actin rings by proline-rich tyrosine kinase 2 interacting with gelsolin. *J. Cell Biol.* **160,** 565–575 (2003).
29. Niwa, H., Yamamura, K. & Miyazaki, J. Efficient selection for high-expression transfectants with a novel eukaryotic vector. *Gene* **108,** 193–199 (1991).
30. Saito, T. & Nakatsuji, N. Efficient gene transfer into the embryonic mouse brain using *in vivo* electroporation. *Dev. Biol.* **240,** 237–246 (2001).
31. Richards, L. J., Koester, S. E., Tuttle, R. & O'Leary, D. D. Directed growth of early cortical axons is influenced by a chemoattractant released from an intermediate target. *J. Neurosci.* **17,** 2445–2458 (1997).
32. Finger, J. H. *et al.* The netrin 1 receptors Unc5h3 and Dcc are necessary at multiple choice points for the guidance of corticospinal tract axons. *J. Neurosci.* **22,** 10346–10356 (2002).

nature cell biology

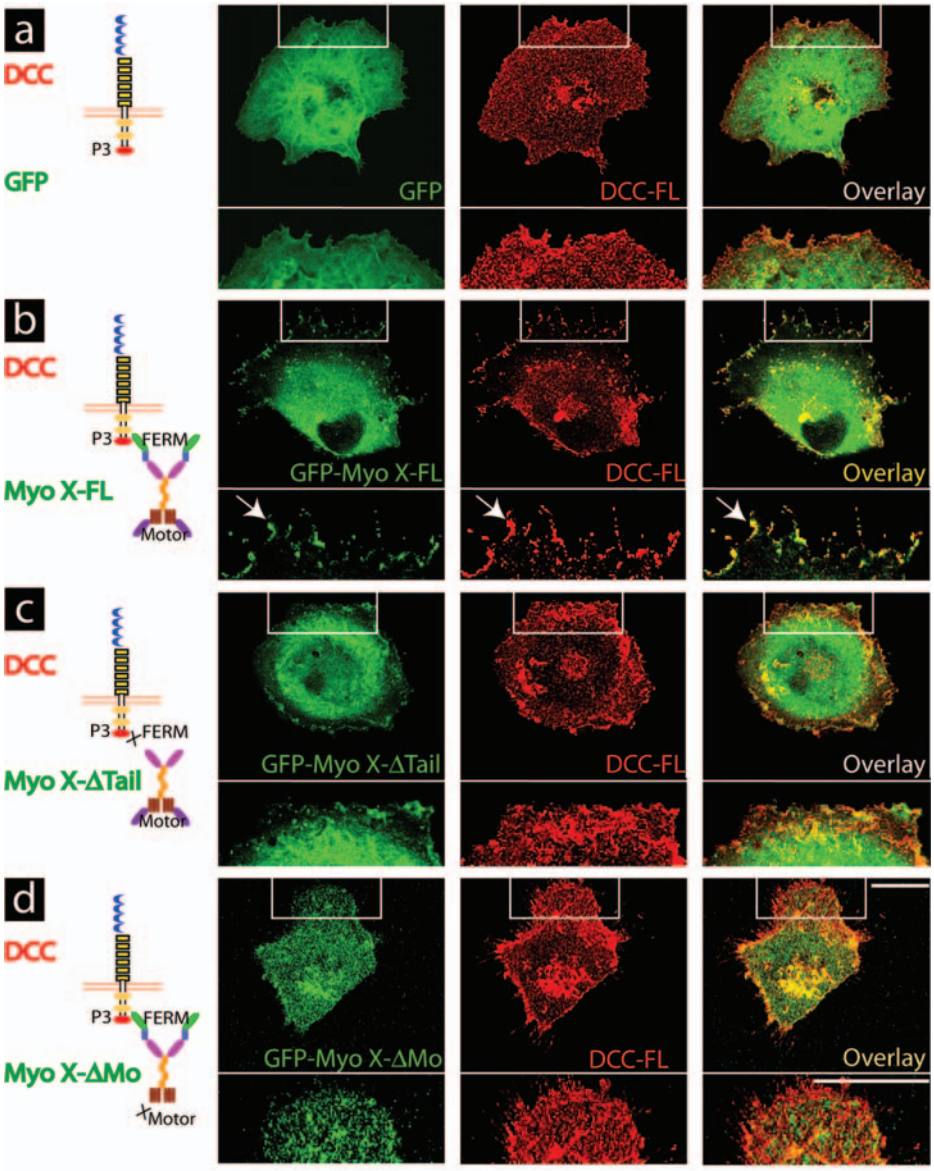

Figure S1 Myo X regulation of DCC localization in a manner dependent on their interaction. Cos-7 cells were transfected with Myc-tagged DCC and the empty vector pEGFP **(a)**, GFP fusion proteins of full-length Myo X (GFP-Myo X-FL)**(b)**, Myo X without the FERM domain (GFP-Myo X-ΔTail)**(c)**, or Myo X without the motor domain (GFP-Myo X-ΔMo)**(d)**. Transfected cells were fixed and stained with antibodies against Myc (red) for DCC expression. GFP (green) indicated Myo X expression. Images indicated in the square boxes were magnified and shown in bottom panels. DCC-Myo X colocalizing puncta were indicated by arrows. Bars, 50 μm.

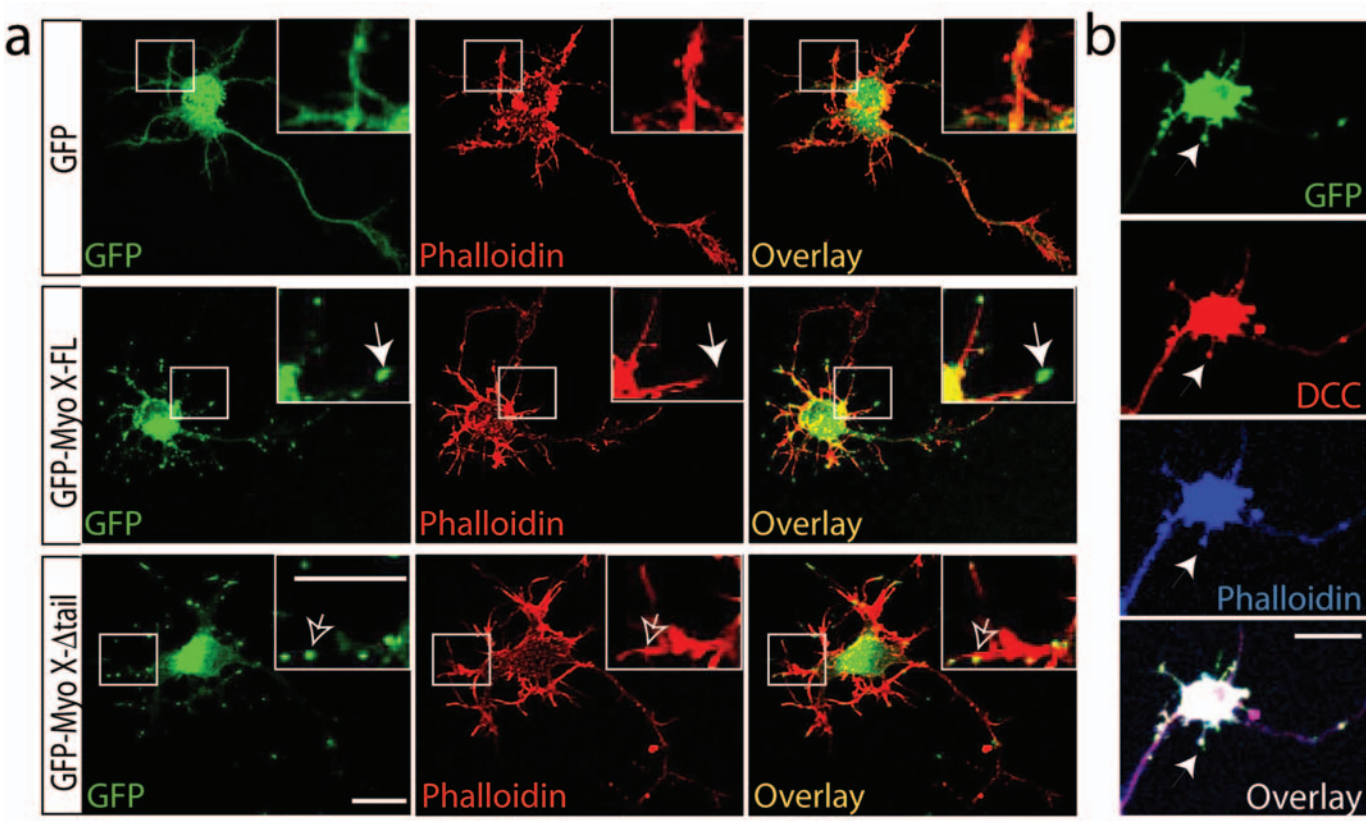

Figure S2 Myo X targeting DCC to the tips of filopodia of neurons. **(a)** Myo X localization at the tips of filopodia of neurons. Rat cortical neurons transfected with indicated plasmids were stained. Phalloidin (red) labeled filopodia, and GFP (green) indicated expression of GFP or GFP-fused Myo X proteins. Images indicated with the square boxes were magnified and shown in inserts. Myo X puncta were indicated by arrows. Bars, 50 μm. **(b)** Myo X targeting DCC to the tips of filopodia of neurons. GFP-Myo X-FL transfected rat cortical neurons were fixed and stained with anti-DCC antibody (red), phalloidin (blue)(to label filopodia/actin filaments), and GFP (green)(to indicate the exogenous GFP-Myo X). Arrows indicate that DCC was co-localized with Myo X at the tips of filopodia (labeled by phalloidin). Bar, 50 μm.

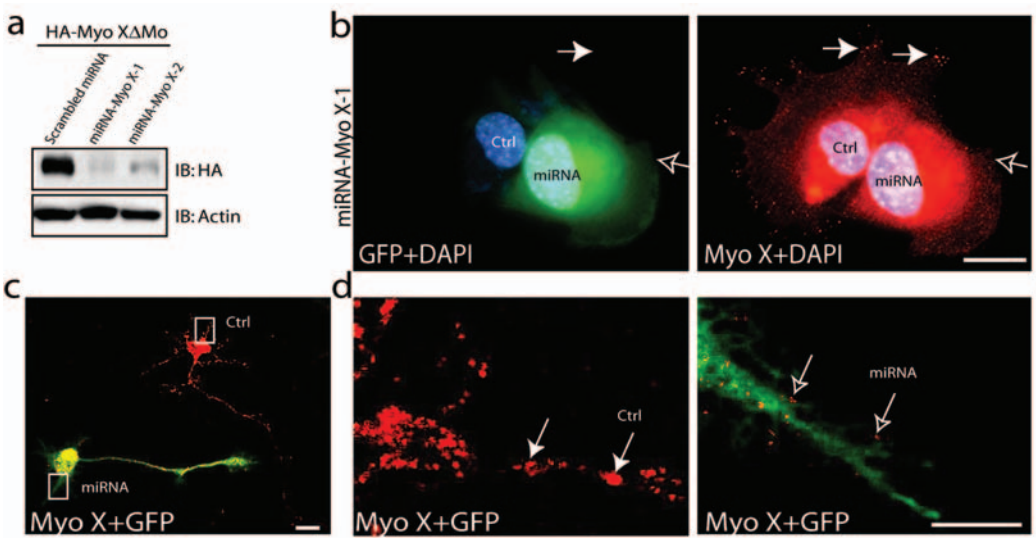

Figure S3 Suppression of Myo X expression by miRNA-Myo X. **(a)** Western blot analysis showing Myo X expression in Cos-7 cells transfected with indicated plasmids. **(b)** Expression of endogenous Myo X was suppressed by miRNA-Myo X in transfected NLT cells. **(c)** Expression of endogenous Myo X was suppressed by miRNA-Myo X in transfected rat cortical neurons. **(d)** Higher magnification of images indicated in the boxes of (c). Bars, 50 μm.In (b) and (c), cells were transiently transfected with miRNA-Myo X plasmid, which encodes GFP as well as miRNA of Myo X. Transfected cells were fixed and immunostained with anti-Myo X antibody (rabbit polyclonal)(red). GFP (green) indicates the expression of the miRNA-Myo X plasmid. Filled arrows indicated Myo X distribution in untransfected cells, and open arrows indicated reduced Myo X expression in miRNA-Myo X transfected cells.

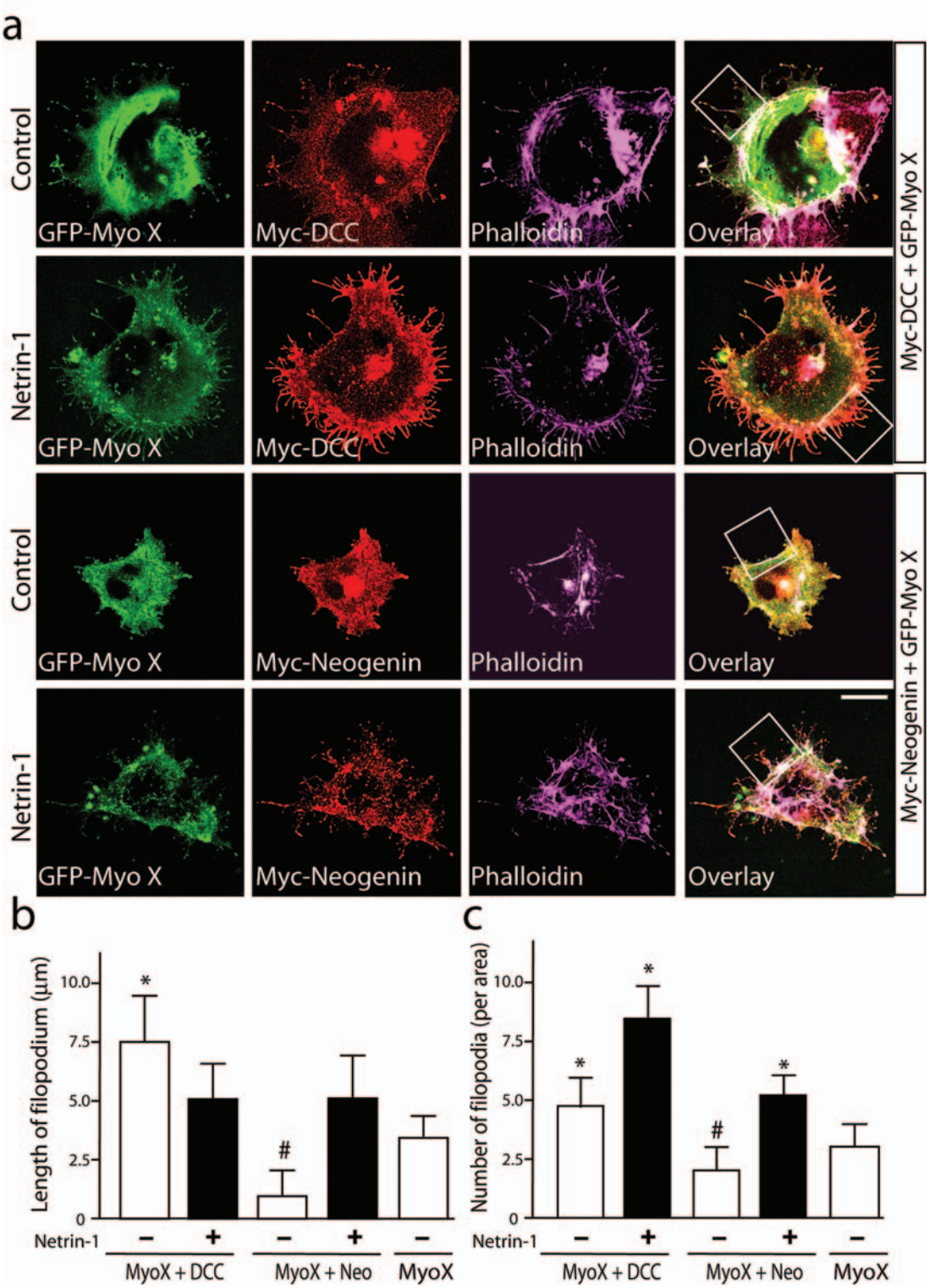

Figure S4 Distinct regulation by DCC and neogenin of Myo X-mediated filopodium elongation in Cos-7 cells. **(a)** Cos-7 cells were transfected with GFP-Myo X without or with DCC or neogenin. Transfected cells were plated onto collegen-coated coverslips for 3 h, and treated with or without netrin-1 medium for 30 min. Cells were stained for DCC (red) and phalloidin (purple). GFP indicated Myo X expression. Bar, 50 µm. **(b-c)** Quantification of filopodial lengths (b) and numbers (c) in Cos-7 cells transfected with indicated plasmids. Data were presented as means ± SEM (n = 30). *, $p < 0.05$, and #, $p < 0.05$, in comparison with cells expressing Myo X alone (*t*-test).